N90-26225

TDA Progress Report 42-101

May 15, 1990

Design and Performance Analysis of the DSS-13 Beam Waveguide Antenna

T. Veruttipong, W. Imbriale, and D. Bathker
Ground Antenna and Facilities Engineering Section

A new 34-m research and development antenna is currently being constructed prior to introducing beam waveguide (BWG) antennas and Ka-band (32 GHz) frequencies into the NASA/JPL Deep Space Network. The new 34-m antenna, fed with either a center or bypass BWG, will lose less than 0.2 dB (excluding surface root mean square and mirror misalignment losses), as compared with a standard-fed Cassegrain antenna at X- (8.4 GHz) and Ka-bands. The antenna is currently under construction and is scheduled to be completed in July 1990. Phase 1 of the project is for independent X- and Ka-band receive-only tests. Phase 2 of the project is for simultaneous S- (2.3 GHz) and X-band or X- and Ka-band operation, and the design is currently under way.

I. Introduction

Feeding a large low-noise, ground-based antenna via a beam waveguide (BWG) system has several advantages over placing the feed directly at the focal point of a dual-reflector antenna. For example, significant simplifications are possible in the design of high-power, water-cooled transmitters and low-noise cryogenic amplifiers, since these systems do not have to rotate, as in a normally fed dual reflector. Furthermore, these systems and other components can be placed in a more accessible location, which leads to improved service and availability. Also, the losses and noise degradation associated with rain on the feedhorn radome are eliminated because the feedhorn can be sheltered from the weather.

The design of the new 34-m BWG antenna at DSS 13 is based upon geometrical optics (GO) criteria introduced by Mizusawa and Kitsuregawa in 1973 [1], which guarantee a perfect image from a reflector pair. Since it may be desirable to retrofit existing antennas with a BWG, as well as construct new antennas, there are two independent BWG designs built into the research and development antenna. The first, termed a bypass design, places the BWG outside one of the elevation bearings on the rotating azimuth platform, thereby retaining the existing elevation wheel and counterweight subassembly, suitable for retrofit applications. The second, a center design, places the BWG through the center of the main reflector, inside the elevation bearings, and through the azimuth axis into a pedestal room located below the antenna. The centerline design is preferred, given new construction. The bypass design uses a pair of paraboloidal sections and two flat mirrors, whereas the center design uses the same four-mirror design (although not physically the same four mirrors) above the azimuth bearing with a flat plate and an ellipsoidal section

that functions as a beam magnifier in the pedestal room. A beam magnifier is required since the pair of paraboloids requires a 29-dBi gain horn to feed, whereas at the lower frequencies a 29-dBi gain horn would be too large to fit in the pedestal room. The ellipsoid design allows the use of smaller 22-dBi gain horns in the pedestal room.

Although the upper four reflectors in either the bypass or centerline BWG satisfy the Mizusawa criteria, the single (curved) ellipsoidal mirror in the pedestal does not. Hence, use of the overall six-mirror, three of which are curved, centerline system introduces a small beam distortion (imperfect imaging). It would require a second ellipsoidal mirror in the pedestal to obtain perfect imaging (in the GO limit). The second ellipsoidal mirror, to be fully compensating for the first, would defeat the (here) necessary beam magnifier function, and is therefore not used.

The microwave antenna gain performance was analyzed using an appropriate combination of physical optics (PO)/spherical wave expansion (SWE) and geometrical theory of diffraction (GTD) software. The initial operation (Phase 1) of the DSS-13 project is for independent X- and Ka-band receive modes, and performance predictions for these frequencies will be given below.

A. Dual-Shaped Reflector Design

The DSN presently operates three 34-m high-efficiency (HEF) dual-shaped reflector antennas with a dual band feed (2.3/8.4-GHz), which has a far-field gain of 22.4 dBi that is conventionally located at the Cassegrain focal point (see Fig. 1). The structures were designed prior to BWG requirements and feature a continuous elevation axle and a carefully designed elevation-wheel substructure. The elevation wheel is supported by an alidade that rotates on a circular azimuth track. To minimize the cost of developing a new 34-m BWG antenna, as much as possible of the existing structure design was to be used (see Fig. 2). Through the use of a clever mechanical design, the elevation-tipping structure was modified to accommodate a central BWG inside the elevation bearings. To provide clear access for an 8-ft (2.44-m) diameter, center-fed BWG, the main reflector backup trusses are connected to a revised elevation wheel via the integral ring girder, or IRG. The IRG is a toroidal structure, an octagonal space truss with a square cross section, approximately 290 in. (~7.4 m) in maximum radius and 80 in. (~2.0 m) high. It is interwoven with, but separate from, the conventional rib-and-ring backup structure. In order to minimize the distortion of the main reflector surface under gravity loading, the reflector connections to the elevation-wheel structure were selected to provide equal stiffness supports. This is achieved by grouping eight equally spaced reflector radial ribs into four pairs and connecting each pair to the IRG top plane at alternate vertices of the octagon. The vertices lying on the elevation axis, however, are reserved for supporting the IRG at the two elevation-bearing points. The counterweight and single elevation bullgear lie on a plane orthogonal to the elevation axis. The entire tipping structure (including the main reflector, elevation wheel, subreflector, and its support) is weight-balanced about the elevation axis.

Selection of the previously designed HEF-reflector structure fixes the focal length/diameter (f/D) of the main reflector surface. The reflector shape is free to be different from the HEF design, but had to be within an adjustable tolerance (~1 in.) of the existing surface to allow use of the existing design drawings.

B. Feed Selection

GO was used to design the upper portion of the centerline BWG system (mirrors M1 to M4). As shown in Fig. 3, the first mirror, M1, has azimuth and elevation rotations together with the main reflector and subreflector. A plane surface is used for M1 to ensure an imaged feed pattern that is independent of the elevation angle of the antenna. Mirrors M2 and M3 are sections of paraboloids, and the system is designed so that a feed placed at F_2 (in the GO limit) is perfectly imaged at F_1.

An imaged feed pattern at F_1 is used to illuminate the subreflector with a narrow-angle high-gain (~29-dBi) pattern. This configuration is used because of the large distance between the subreflector and the first BWG mirror (M1), and also because the size of M1 (as well as M2) is smaller than the subreflector. The position of the focal point F_1 in Fig. 3 must be close to M1 to achieve acceptable spillover losses at the subreflector, as well as M1 and M2. Normally F_1 is in the neighborhood of the main reflector vertex with an 8–9 deg half-cone angle of illumination at the subreflector, as compared with 17 deg for the normal Cassegrain feed of the 34-m HEF antenna.

The diameter of the subreflector D_S is determined by the size of the main reflector. According to [2], a subreflector diameter not exceeding 1/10 of a main reflector is normally selected for good radiation efficiency of the antenna. For a 34-m antenna, a subreflector diameter of 3.43 m (135 in.) was chosen. The illumination angle θ_S is determined next. For the same f/D ratio as the HEF and D_S = 135 in., the distance L_1 = 593.1 in. (~15 m) is obtained. Iterations are needed for a calculation of θ_S and the location of F_1. Known parameters are D_S = 135 in.,

L_1 = 593.1 in., and D_2 = 94 in. (~2.4 m). Variable parameters are 8.0 deg $\leq \theta_S \leq$ 9.0 deg, 105 in. $\leq L_2 \leq$ 110 in. (~2.7 m), and 9.5 deg $\leq \theta_m \leq$ 11.0 deg. The angle θ_m is the illumination angle at M2 with an edge taper of about −23 dB. The results of iterations of GO ray geometry between D_S and D_2 are θ_S= 8.7 deg, θ_m = 10.4 deg, L_0= 441.11 in. (~11.2 m) and L_2 = 108.01 in. (~2.7 m). The GO focal length of M2 is selected as 260 in. (6604 mm). The exact dimensions are somewhat arbitrary, but are constrained by the M2 mirror-projected diameter (96-in. limit). The BWG shroud, or tube diameter, was chosen because the tube effects at S-band would be small. It is now necessary to design a horn that has an approximately −18 to −20-dB taper at 8.7 deg (the illumination of the subreflector) and minimal spillover past 10.4 deg (the illumination of the BWG mirror).

An important design parameter is the horn's flare angle. Figure 4 shows the patterns and efficiencies (spillover times phase efficiency) for several different horn-flare angles and, as can be seen, the patterns are not very sensitive to the flare angle. For that reason and because the JPL standard feedhorn has a flare angle of 6.25417 deg, it was decided to examine the standard flare angle, since existing feedhorns or feedhorn designs could be utilized.

Various horn sizes with the JPL standard angle of 6.25417 deg and frequency = 8.45 GHz were investigated. The goal was to find a horn with a −18-dB taper at θ = 8.7 deg (near-field distance of 425 in., ~10.8 m) and a −23-dB taper at θ = 10.4 deg (near-field distance of 260 in., ~6.6 m). The distances 260 in. and 425 in. are for a high-gain horn illuminating the BWG mirror M2 and the subreflector, respectively. The combined phase and spillover efficiencies ($\eta_{phase} \times \eta_{spill}$) should be optimally between 8.7 and 10.4 deg. The results from various trials show that a 19-in. (~ 483-mm) aperture diameter at X-band, with dimensions shown in Fig. 5, gives a radiation pattern that meets these goals. Figures 6(a) and 6(b) show amplitude, phase, and efficiency plots of the 19-in. X-band aperture diameter at r = 425 in. and 260 in., respectively. From Fig. 6(a), the edge taper at the rim of the subreflector (θ = 8.7 deg, r = 425 in.) is equal to −18.7 dB, which is within the desirable range of −18 dB to −20 dB. The combined phase and spillover efficiency is about 96.4 percent, where the maximum efficiency is about 97.8 percent, at θ =~11.5 deg. This is a typical design point for a dual-shaped system, since the use of the maximum efficiency point results in a larger subreflector. It should be noted that the results for a 21-in. (~533-mm) aperture were very similar to those of the 19-in. aperture, but the 21-in. aperture results in a horn that is 11 in. (~280 mm) longer at X-band; hence, the smaller design was chosen.

From Fig. 6(b), the GO edge taper at the rim of any BWG mirror (at r = 260 in.) is ~ −23.6 dB at θ = 10.4 deg, with 96.5 percent efficiency. The maximum efficiency is equal to 96.7 percent at θ = 9.8 deg, which falls between the desired values of 8.7 and 10.4 deg. Because the 19-in. X-band horn has radio frequency (RF) radiation characteristics that meet the requirements, it is therefore used in the design of BWG mirrors and synthesis of dual-shaped reflectors.

In similar analyses, the +22-dbi horn required for the F_3 pedestal room focus was examined at a range of 165 in., as discussed in section I.D.

C. Dual-Shaped Reflector Design

An essential requirement of the 34-m main reflector is to maintain the newly designed BWG antenna surface contour within ±0.5 in. (13 mm) of the previously designed HEF antenna. This makes it possible to retain the existing backup structure and adjust the individual reflecting panels with existing standoffs to fit the newly designed contour.

The X-band feedhorn pattern at r = 425 in. (the mean distance to the subreflector) is used as an input pattern to a high-resolution synthesis program developed by Galindo-Israel.[1] The input parameters were similar to the HEF antenna design and are shown in Figs. 7(a), 7(b), and 7(c). The maximum difference between the main reflector surfaces of DSS 13 and the HEF antenna is 0.43 in. (11 mm), allowing HEF antenna panel forming tooling and standoff hardware to be reused.

D. Center-Fed BWG

This section provides technical details for the design of the centerline BWG feed system (Fig. 3). GO was used to design the centerline system of the first four mirrors (M1 to M4), while PO was applied to the design of the curved mirror (M5) in the pedestal room. As shown in Fig. 3, the first mirror, M1, has azimuth and elevation rotations together with the main reflector and subreflector. A plane surface is used for M1 to ensure an imaged feed pattern that is independent of the elevation angle of the antenna. Mirrors M2, M3, and M4 are attached to that part of the structure with azimuth rotation only. The last two mirrors, M5 and M6, are stationary on the ground in the pedestal room.

[1] V. Galindo-Israel, "Circularly Symmetric Dual-Shaped Reflector Antenna Synthesis With Interpolation Software-User Manual" (internal document), Jet Propulsion Laboratory, Pasadena, California, January 1988.

For a long RF ray path, curved mirrors are needed to refocus and guide energy from F_1 to F_2 (and later on to F_3) with acceptable spillover loss. It is preferable to have two curved mirrors arranged so that Mizusawa's conditions [1] are met, thus achieving minimum cross-polarization at high frequency. Oversize flat plates are used merely to direct the RF beam into desired directions without changing any other characteristic of the RF beam.

The choice of two identical paraboloidal sections for M2 and M3 has the following advantages:

(1) In the GO limit, a circularly symmetric input pattern still retains the original symmetrical shape after reflection through both (or all four) surfaces.

(2) Since there is no focal point between the two curved mirrors, as there would be with ellipsoids, RF performance is not sensitive to the spacing (L_3) between the two mirrors, provided that the spillover loss remains small.

(3) A high-pass (filter) RF performance is obtained with very good X-band performance for 8-ft mirrors (<0.1 dB for this path).

(4) It is possible to have four identical mirrors (two for center-fed and two for bypass) when paraboloidal surfaces are used in the design.

(5) Identical mirrors are obviously more economical.

The centerline BWG paraboloidal mirrors are positioned so that feedhorns and instrumentation packages can be either in an alidade location (not presently planned for implementation) or the pedestal room. Spacing between the two paraboloids, L_3 = 360 in. (~9144 mm), is chosen to allow enough headroom for vertical orientation of S-, X-, and Ka-band/amplifier subassemblies. Also, the S-band spillover loss at this distance is acceptably small. A flat plate, M4, reflects the RF beam downward along the antenna azimuth axis to the pedestal room, with focal point F_2 about 85 in. (~2 m) above the azimuth floor and about 195 in. (~5 m) above the pedestal room ceiling.

A significant decision was whether to locate the feeds on the alidade at focal point F_2 (requiring 29-dBi gain feeds) or in the pedestal room under the antenna, using focal point F_3. Despite an additional RF loss going from F_2 to F_3, the clear advantages of using the pedestal room (more available space, no cable wrap across the azimuth axis, smaller feeds required, etc.) led to its selection. The stable environment of the pedestal room was a major determinant.

Only X- and Ka-bands are planned for Phase I operation of DSS 13. However, the design must have capabilities for future S/X-, X/Ka-, C-, and Ku-band operations (S-band is 2 GHz, C-band is 4–6 GHz, and Ku-band is 13–15 GHz). Low-gain horns (~22 dBi) are desirable for all frequency bands. A basic layout for the RF design in the pedestal room is given in Fig. 2. Mirror M5 is an ellipsoidal surface used for magnifying gain (reducing beamwidth) from 22 to 29 dBi and switching among various horns by rotating M5 about the antenna aximuth. Mirror M6 is a flat plate used to reflect the RF beam from a vertically positioned feedhorn to M5, with an angle θ = 60 deg. The 60-deg angle is preferred because the existing JPL dichroic plate is designed with a 30-deg incident angle (equivalent to θ = 60 deg). Therefore, the θ = 60 deg angle will be convenient for simultaneous operation (S/X- and X/Ka-band) while reusing the existing JPL dichroic technology. Even though a smaller angle of θ would yield a more symmetric beam pattern, angles smaller than 50 deg will have shadowing problems among M5, M6, and the feedhorn. The curvature of M5 is determined by placing the near-field phase center of the 22-dBi X-band horn at a focal point of M5 (F_3) and calculating the field at M3 by using PO. Iteration continues by changing the surface curvature of M5 until the scattered field has an average edge taper at M3 of about −23 dB. The mirror M5 is adjusted vertically until the best-fit phase center of the scattered field of M5 overlays F_2. The curvature and position of M5 are designed at X-band, and there is no vertical adjustment of the mirror for other bands. The Ka-band horn (or other high-frequency horns) must be defocussed and the gain increased slightly (from 22 to 23 dBi) to approximate the same edge taper and best-fit phase center as at X-band. The detailed RF design layouts in the pedestal room for X- and Ka-bands are shown in Figs. 8 and 9. There are small lateral translations of the feedhorns to compensate for radiation pattern asymmetry due to the surface curvature of mirror M5.

The theoretical performance of the BWG system is determined by using various combinations of analytical software, as described in [3] and [4]. Figure 10 shows the measured pattern of the input of the 22-dBi horn fed at F_3, the calculated output of the ellipsoid at F_2, and demonstrates the X-band gain-magnifying (beamwidth-reducing) property of the ellipsoid. Figure 11 shows the X-band output of the BWG at F_1 compared with both the calculated input at F_2 and the measured 29-dBi horn. Figure 12 shows a comparison of the E- and H-planes of the BWG output. The system is designed to image the 29-dBi horn of Fig. 5 at the input to the dual-reflector system. Figure 13 shows the input and output of the BWG at Ka-band and illustrates the nearly perfect imaging properties of the

paraboloid pair. Figure 14 is a comparison of the 29-dBi horn and the BWG feed for the dual-reflector system at X-band.

E. Bypass BWG Design

A general layout of the bypass BWG is shown in Fig. 15(a). All mirrors rotate in the elevation plane except M10. To allow enough clearance between mirror M10 and the elevation bearing, a bypass BWG vertical tube must be positioned at Hoop 6, which is about 403 in. (~10.2 m) from the antenna center line. A retractable flat plate, M7, is out when the center-fed BWG mode is used. Mirrors M8 and M9 are paraboloidal surfaces positioned to satisfy Mizusawa's conditions. The mirrors M7, M8, and M9 are attached to and move together with the main reflector structure. A flat mirror, M10, is attached to an elevation bearing; it is not rotated with elevation rotation (but moves with azimuth rotation) in order to have a focal point F_4 always pointing straight downward to the alidade platform. By carefully adjusting L_5 and L_6 so that the distance from F_1 to the mirror M8 is equal to 260 in. (6604 mm), the paraboloidal mirrors M8 and M9 are identical to the mirrors M2 and M3 in the center-fed BWG design. Thus, there are four identical curved mirrors in this double BWG feed system.

The value of L_5 used in this design is 290.645 in. (7382 mm), which is the same as the spacing between mirrors M8 and M9. There is also enough clearance between an incident ray at the lower rim of M8 and the rim of the opening hole on the surface of the main reflector. Figure 15(b) shows detailed dimensions of the bypass BWG design. Observe that the bypass performs slightly better than the center BWG, due to the absence of the ellipsoidal magnifier mirror and the shorter main path (290 versus 360 in.).

F. Microwave Performance Summary

Table 1 lists the BWG losses at X- and Ka-band for both BWG systems and shows the reference HEF performance. The loss due to spillover was calculated with the assumption that the mirrors are in free space and that the energy not impinging on the mirrors is lost.

II. Conclusions

The new 34-m antenna fed with either a center or bypass BWG will lose 0.2 dB or less, as compared with a standard-fed Cassegrain antenna at X- and Ka-bands. The antenna is currently under construction and is scheduled to be completed in July 1990. Phase 1 of the project will provide independent X- and Ka-band receive-only operation. Phase 2 of the project will provide for simultaneous S- and X-band or X- and Ka-band operation, and the design is currently under way.

Acknowledgments

The authors would like to thank M. Esquivel for calculating the horn patterns and J. Cucchissi for supplying information on the IRG. J. Withington supplied highly accurate and crucial experimental checks of BWG performances by use of a 1/4 scale model and special data recording and analysis techniques. We would also like to thank the JPL Supercomputing Project for computer time on the Cray X-MP/18.

References

[1] M. Mizusawa and T. Kitsuregawa, "A Beam Waveguide Feed Having a Symmetric Beam for Cassegrain Antennas," *IEEE Trans. Antennas and Propagat.*, vol. AP-21, pp. 884–886, November 1973.

[2] M. Mizusawa, "Effect of Scattering Pattern of Subreflector on Radiation Characteristics of Shaped-Reflector Cassegrain Antenna," *Trans. IECE,* vol. 52-B, Japan, pp. 78–85, February 1969.

[3] T. Veruttipong, J. Withington, V. Galindo-Israel, W. A. Imbriale, and D. A. Bathker, "Design Considerations for Beam Waveguide in the NASA Deep Space Network," *IEEE Trans. Antennas Propagat.*, vol. AP-36, pp. 1779–1787, December 1988.

[4] V. Galindo-Israel, T. Veruttipong, and W. Imbriale, "GTD, Physical Optics, and Jacobi-Bessel Diffraction Analysis of Beam Waveguide Ellipsoids," *IEEE AP-S International Symposium Digest,* vol. 2, Philadelphia, Pennsylvania, pp. 643–646, June 1986.

Table 1. Beam waveguide performance*

Frequency, GHz	Gain, dBi (100 percent efficient)	HEF Cassegrain	DSS-13 Bypass BWG		DSS-13 Center-fed BWG		
		Gain, dBi	Gain, dBi	Portion due to spillover	Gain, dBi	Paraboloid spill portion	Ellipsoid spill portion
8.45 X-band	69.57	69.21	69.13	−0.06	69.06	−0.05	−0.06
31.4 Ka-band	80.98	80.62	80.55	−0.06	80.42	−0.03	−0.03

*Losses due to surface rms, BWG mirror misalignments, subreflector support blockage, and feed system I^2R are not included.

ORIGINAL PAGE
BLACK AND WHITE PHOTOGRAPH

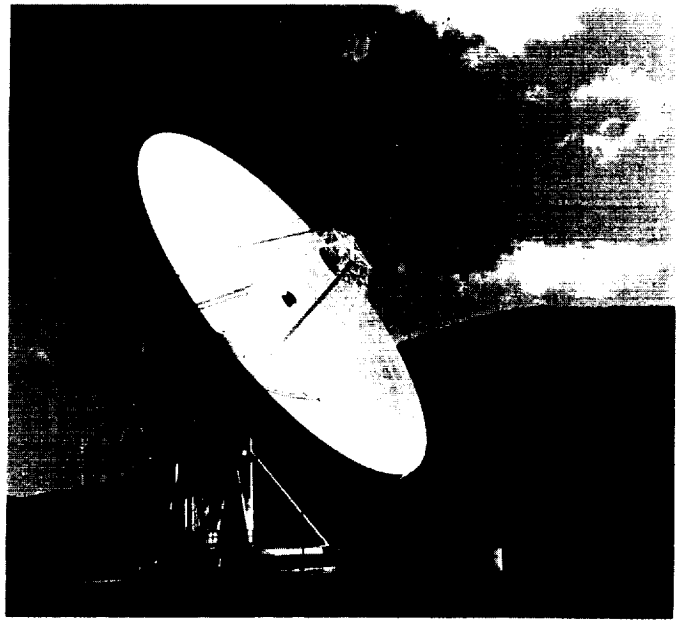

Fig. 1. The 34-m high-efficiency-frequency antenna.

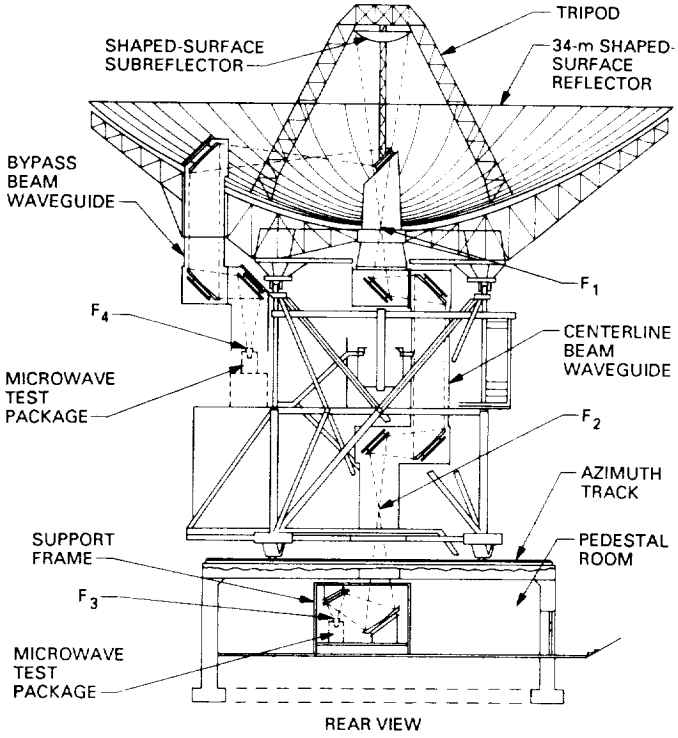

NOTE: IN THIS CONFIGURATION, THE BYPASS BWG IS ACTIVE

Fig. 2. New 34-m beam waveguide antenna.

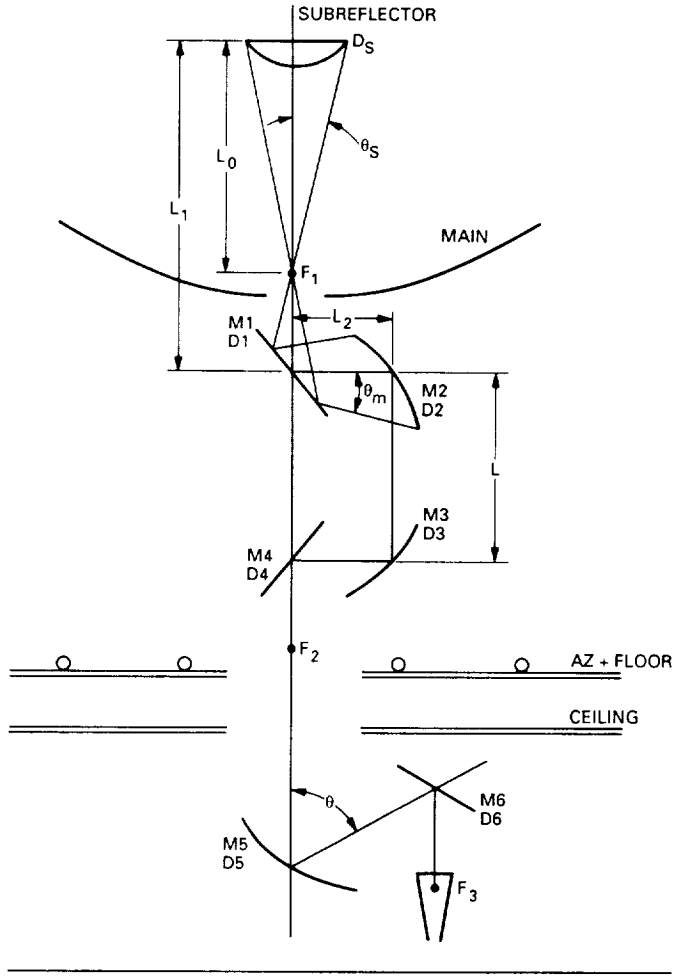

Fig. 3. A center-fed beam waveguide layout.

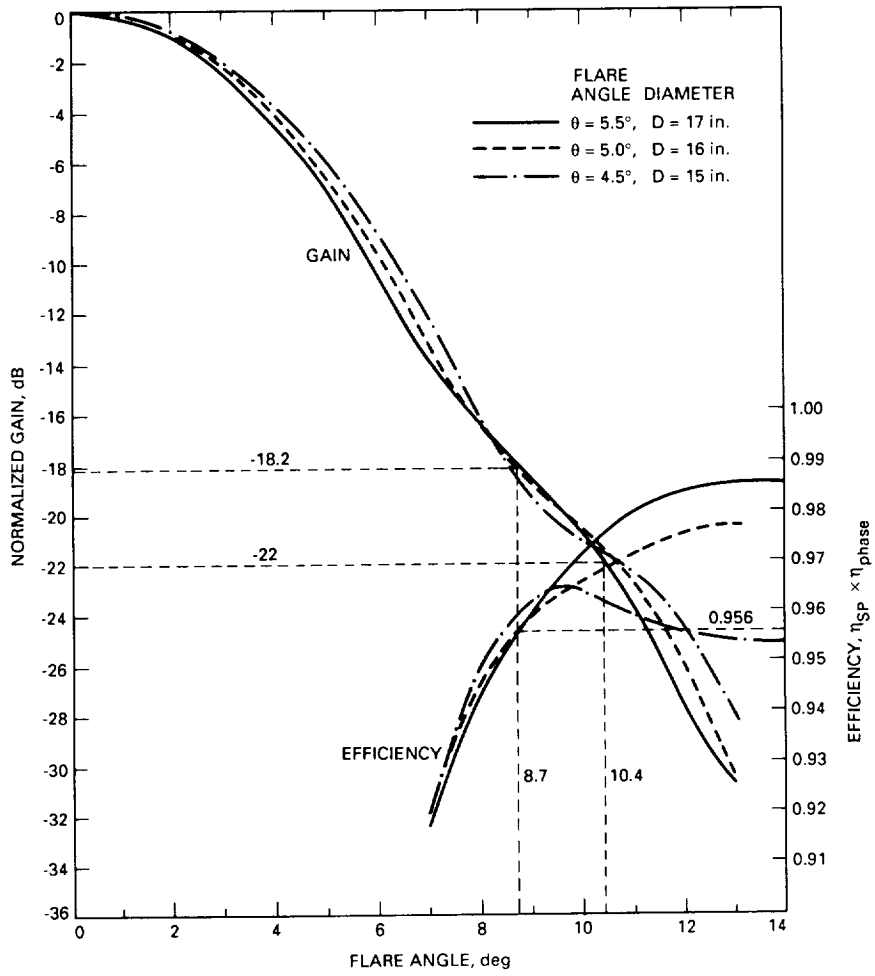

Fig. 4. Gain and efficiency versus flare angle.

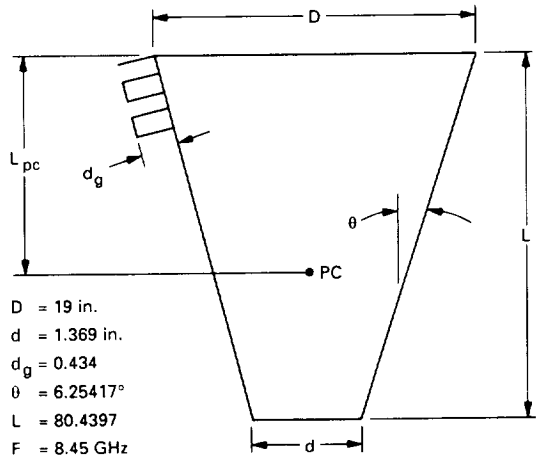

Fig. 5. Horn dimensions.

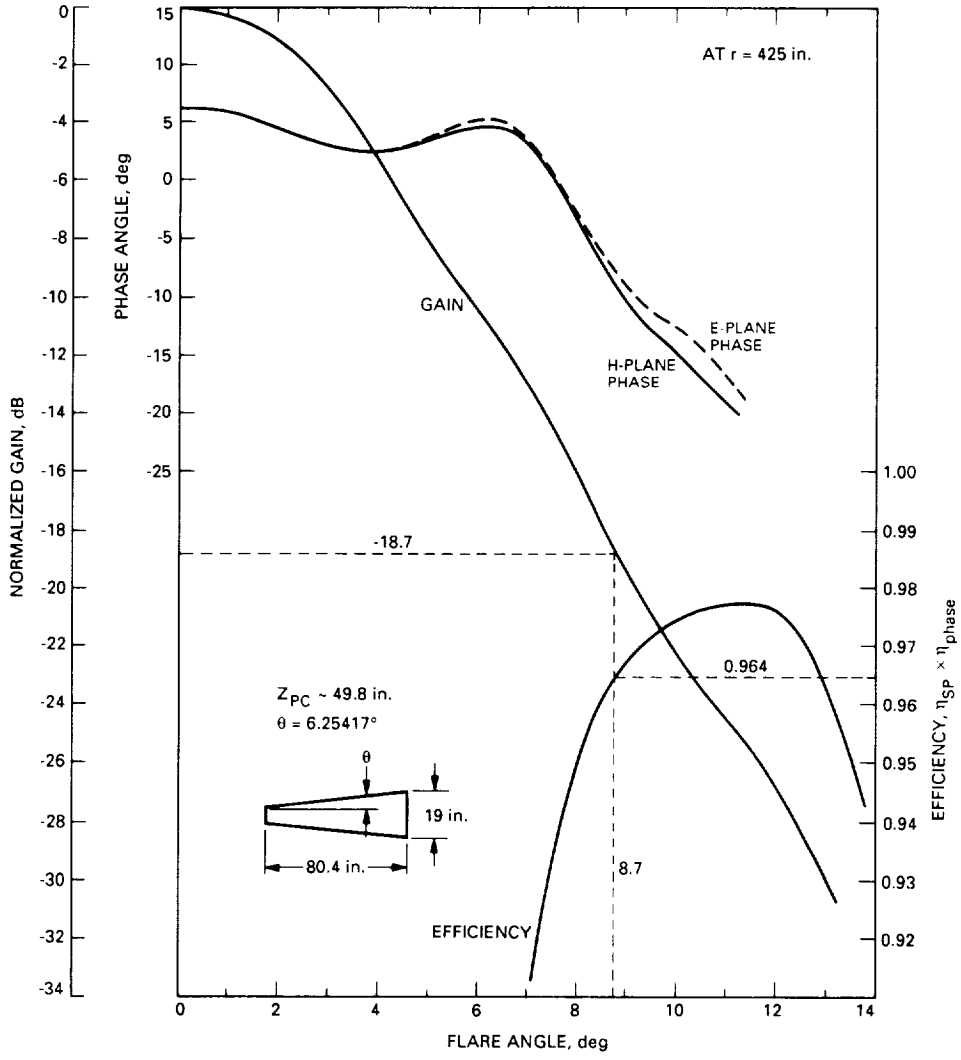

Fig. 6(a). Horn selection study (at r = 425 in., subreflector), existing JPL flare angle.

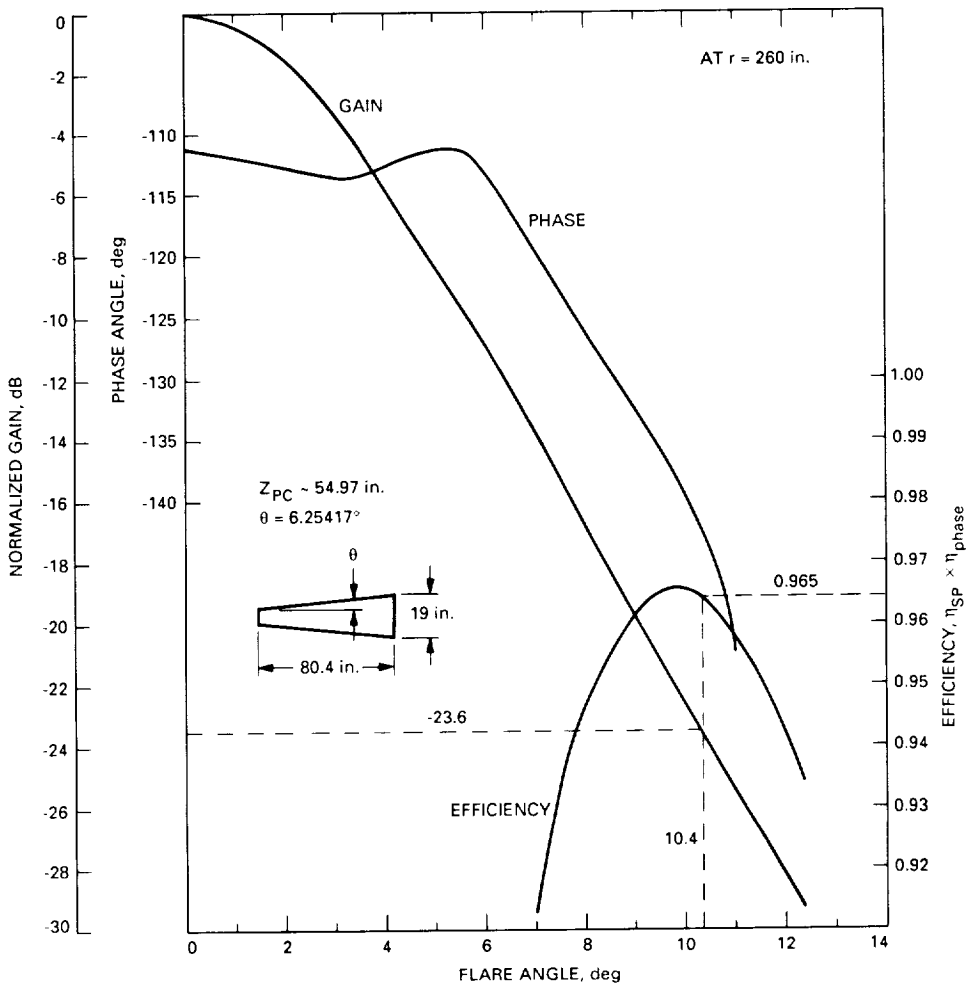

Fig. 6(b). Horn selection study (at r = 260 in., beam waveguide), existing JPL flare angle.

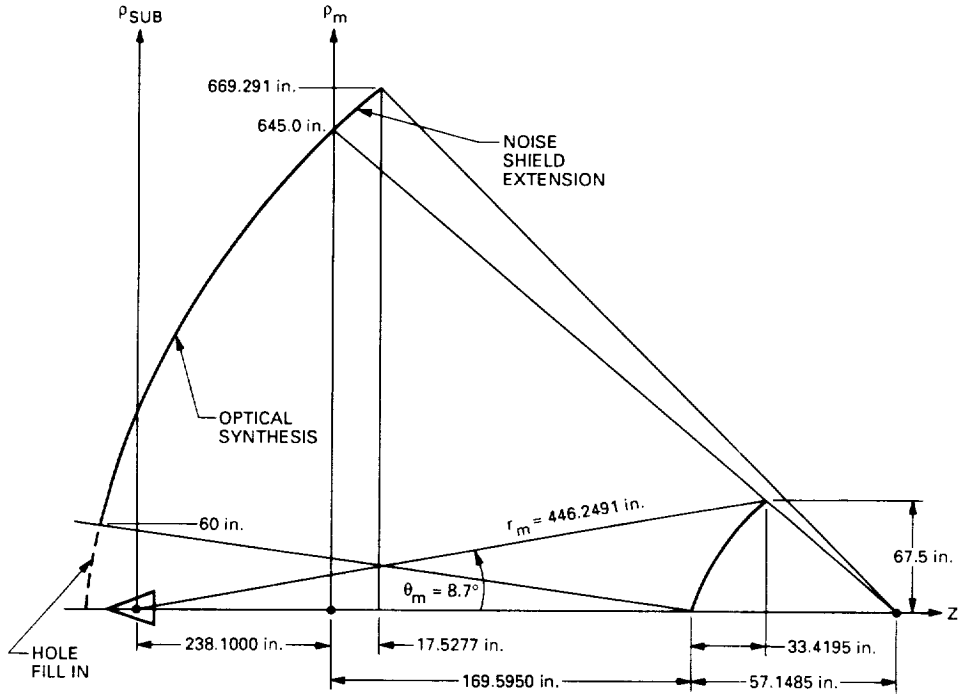

Fig. 7(a). The 34-m beam waveguide antenna geometrical synthesis parameters.

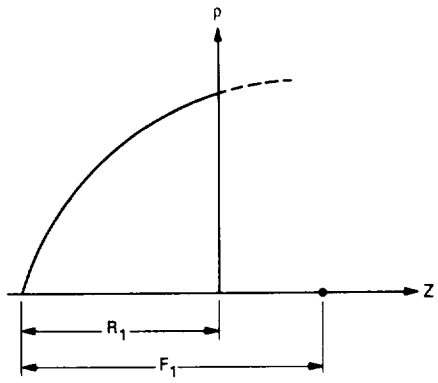

$$Z_{Noise} = -R_1 + \frac{\rho^2}{4F_1};\ R_1 = 228.48 \text{ in.},\ F_1 = 455.22 \text{ in.}$$

Fig. 7(b). Equivalent paraboloid for the noise shield.

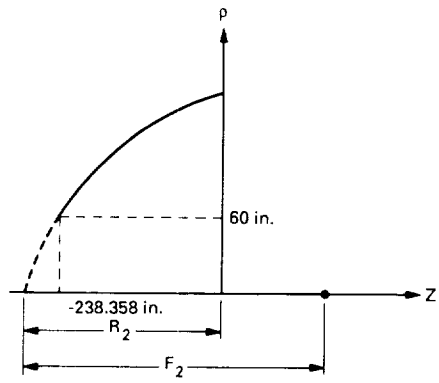

$$Z_{Hole} = -R_2 + \frac{\rho^2}{4F_2};\ R_2 = 240.55 \text{ in.},\ F_2 = 410.14 \text{ in.}$$

Fig. 7(c). Equivalent paraboloid for the hole.

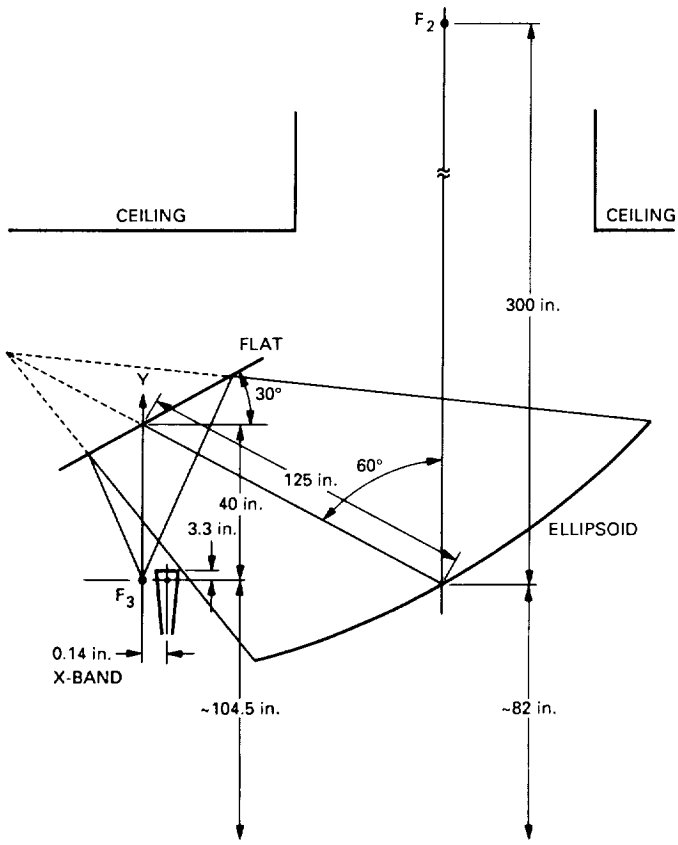

Fig. 8. Pedestal feed system for X-band.

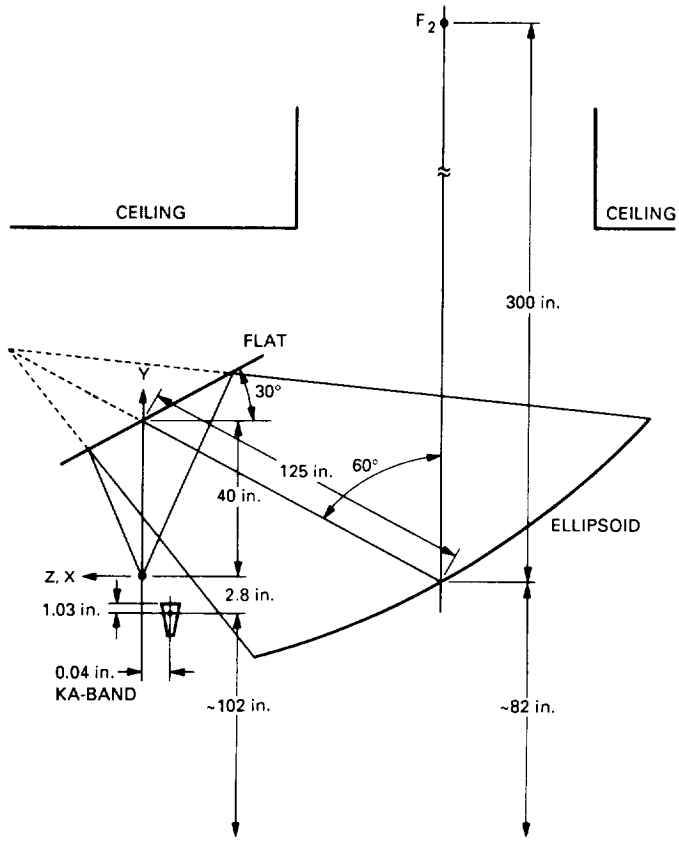

Fig. 9. Pedestal feed system for Ka-band.

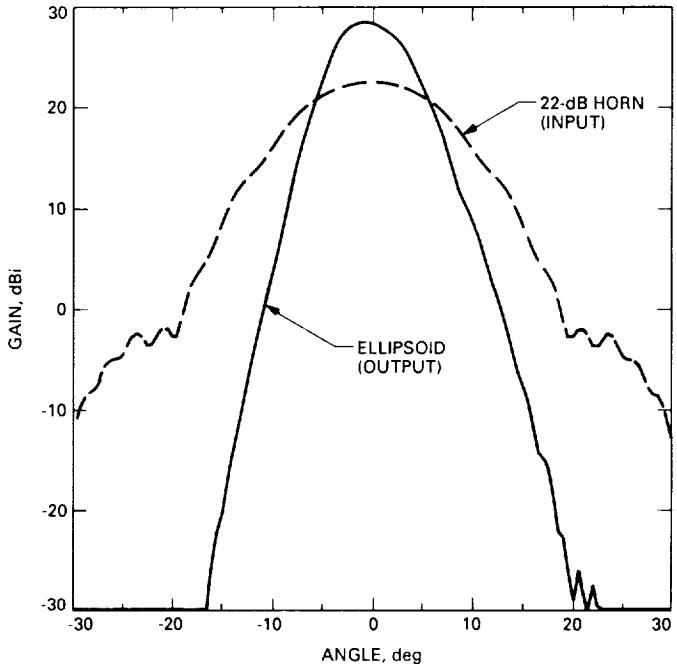

Fig. 10. Beam magnifier ellipse.

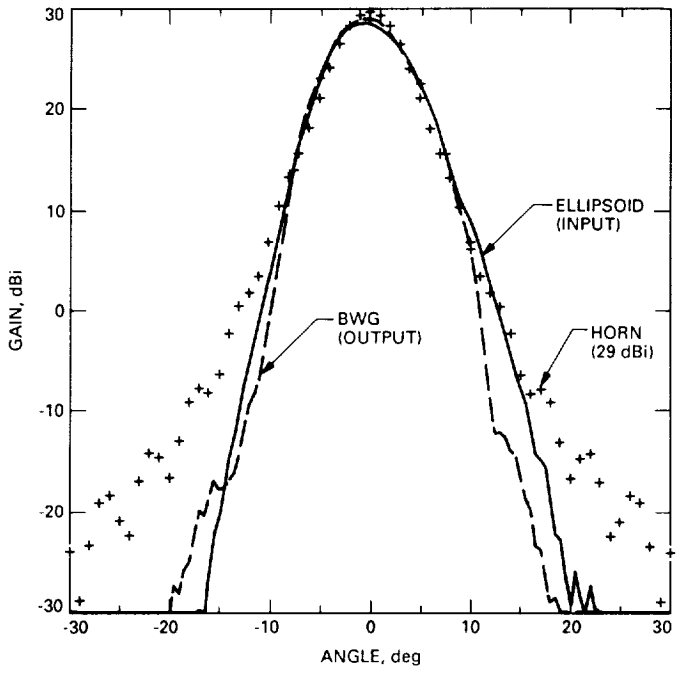

Fig. 11. Center-fed output beam waveguide.

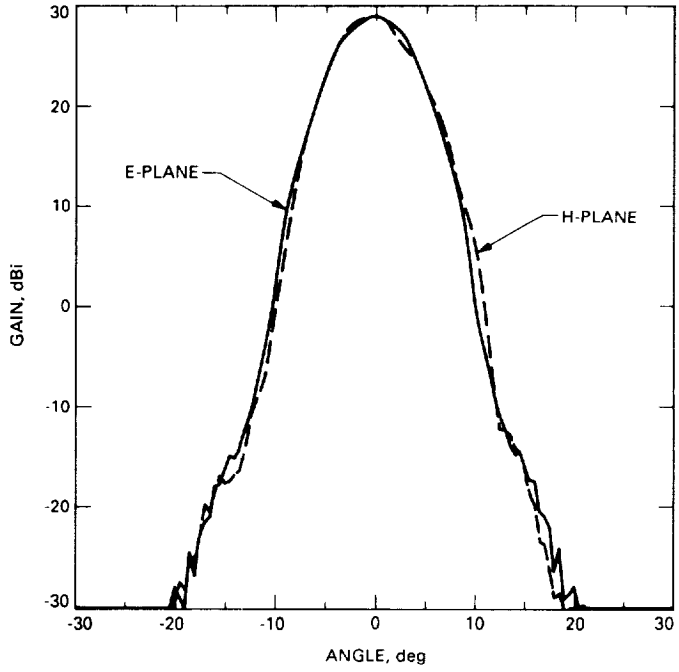

Fig. 12. X-band E- and H-plane beam waveguide output.

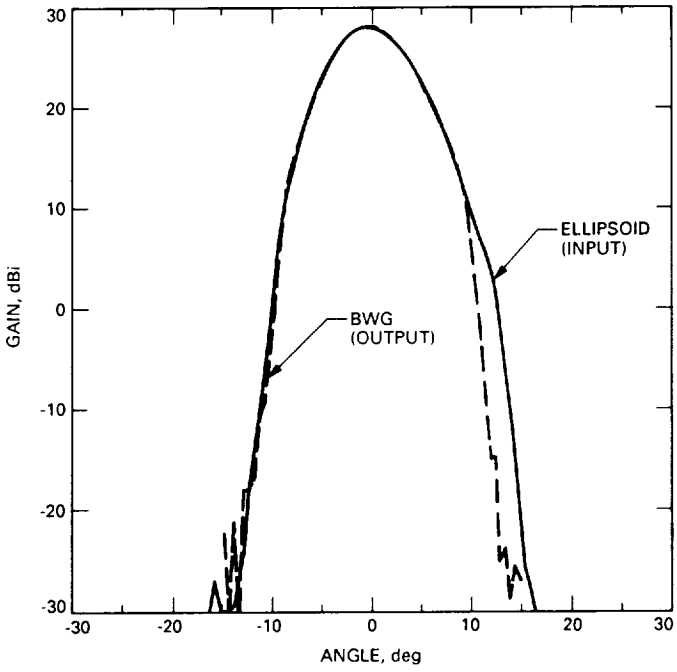

Fig. 13. Center-fed beam waveguide output (Ka-band)

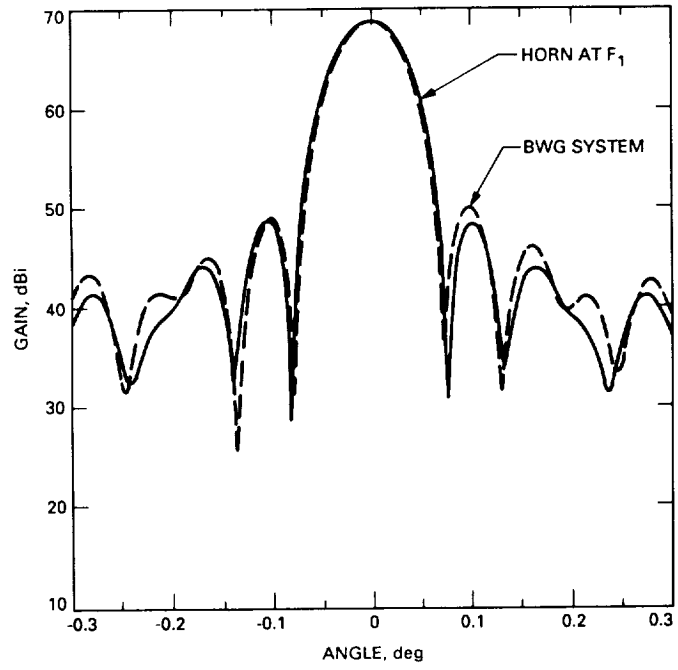

Fig. 14. Comparison of horn versus beam waveguide feeding dual-reflector system.

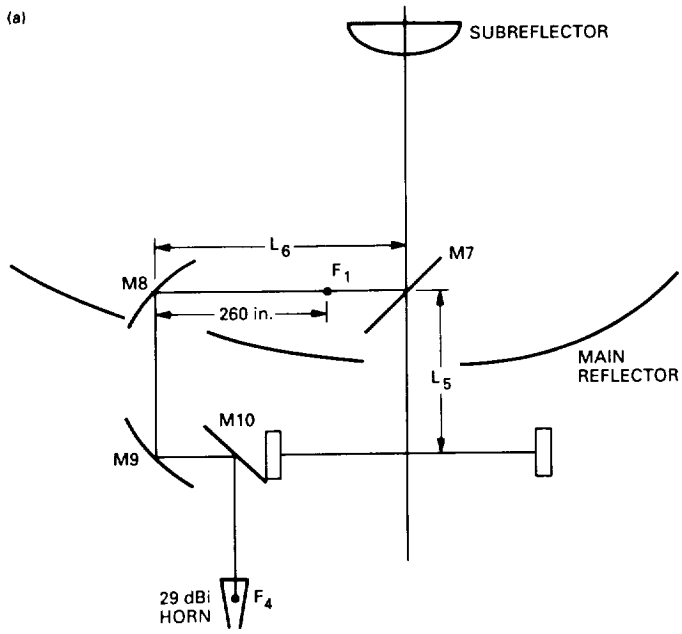

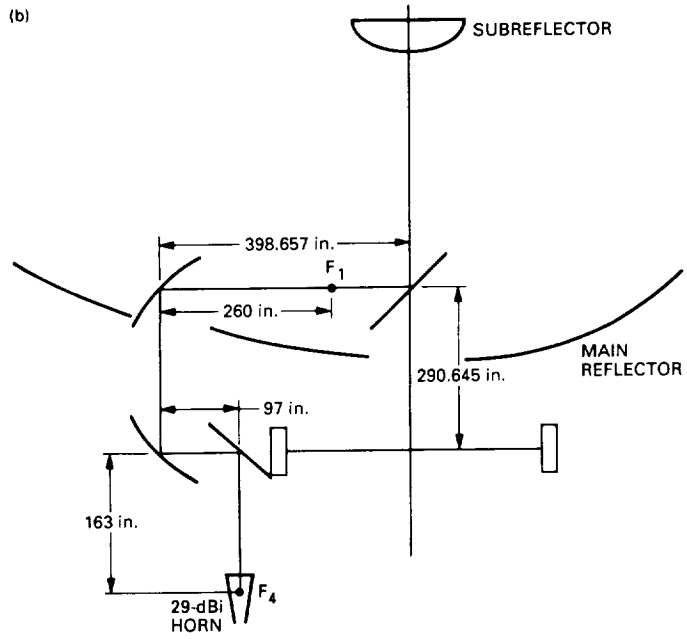

Fig. 15. Bypass beam waveguide geometry: (a) general layout; (b) detailed dimensions of the bypass beam waveguide design.